Pergamon

0967-0637(95)00068-2

Deep-Sea Research I, Vol. 42, No. 9, pp. 1521–1543, 1995

0967-0637/95 $9.50 + 0.00

Surface mixed and mixing layer depths

KEITH E. BRAINERD and MICHAEL C. GREGG

(*Received* 29 *August* 1994; *in revised form* 6 *February* 1995; *accepted* 30 *March* 1995)

Abstract—In order to understand the daily cycle of heat storage within the surface mixed layer it is necessary to distinguish between the mixed layer, the zone of relatively homogeneous water formed by the history of mixing, and the mixing layer, the zone in which mixing is currently active. We compare surface layer definitions based on density (or temperature) with turbulence measurements to evaluate their skill in finding mixed and mixing layer depths, using definitions based on density increase from the surface, and on density gradients. Both types of definition are capable of finding the mixed layer depth, with some tuning for local conditions. Neither definition, however, gives mixing layer depths consistently matching the turbulence measurements, although density differences give more stable results. Measurements of turbulent dissipation rates or overturning length scales often yield consistent estimates of mixing layer depths, but there are cases where overturning lengths give distinctly better results. We conclude that overturning length scales give the most reliable measure of mixing layer depth, although conventional shipborne CTDs are seldom capable of sufficiently resolving the overturns.

INTRODUCTION

The concept of the surface mixed layer has proven to be useful in many oceanographic contexts, but a wide range of meanings have been attached to it. In this paper we wish to distinguish between the mixing layer, the depth range through which surface fluxes are being actively mixed by turbulent processes, and the mixed layer, the depth range through which surface fluxes have been mixed in the recent past (where recent past often means within the preceding daily cycle, but longer time scales are sometimes more appropriate). This distinction is not new, having been noted in observations (Shay and Gregg, 1986) and models (Woods and Barkmann, 1986). Since then, however, many more observations have been taken, allowing quantitative comparisons of mixing and mixed layer depths.

To identify the mixing layer, we use two measures of turbulence (ε, the rate of viscous dissipation of turbulent kinetic energy, and L_T, the length scale of turbulent overturns). We compare these measures with the signals in temperature and density, in data collected on several cruises using the Advanced Microstructure Profiler (AMP), a free-falling instrument that measures fine-scale profiles of temperature and conductivity, and micro-scale profiles of gradients of temperature and velocity fluctuations, from which we estimate dissipation rates. Because this instrument typically starts each drop within the wake of the ship, the top 10 m of data are contaminated, and cannot be used. In this study

Applied Physics Laboratory and School of Oceanography, College of Ocean and Fishery Sciences, University of Washington, Seattle 98105, U.S.A.

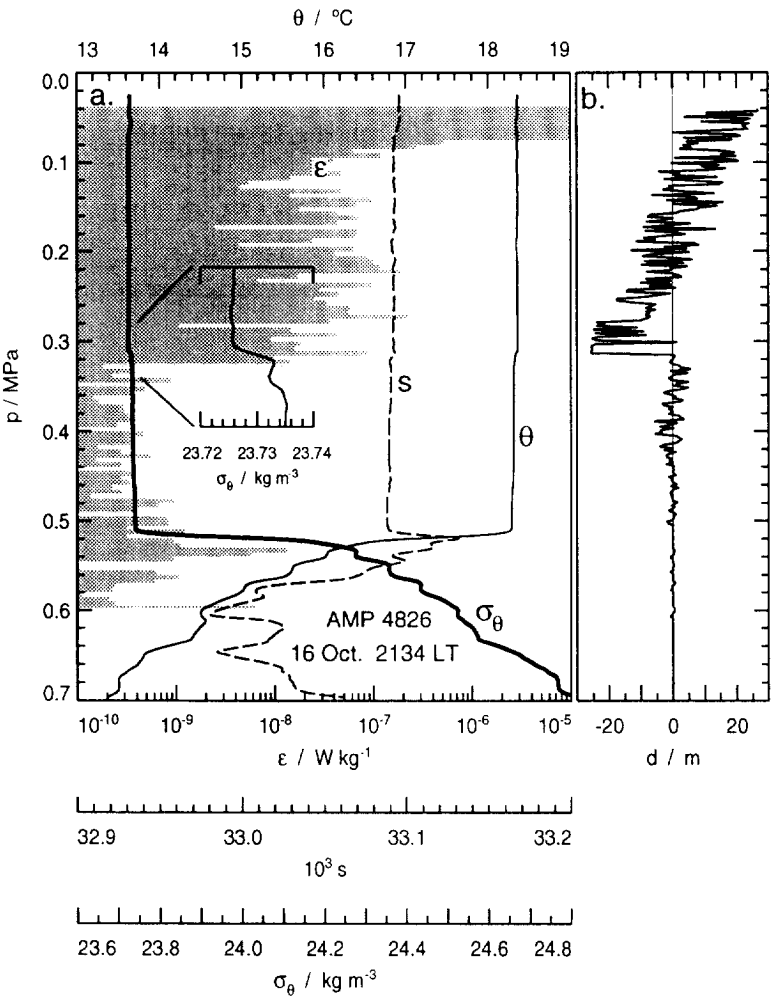

Fig. 1. Profile taken during convective deepening on PATCHEX: 2134 LT (local time, UTC—8 h). Panel a. Profiles of ε, θ, salinity and σ_θ. The shading is ε, estimated in 0.5 m bins; θ and σ_θ have been processed with a 0.8 m triangular filter. The small density step at 0.32 MPa (inset) is the bottom of the mixing layer. Panel b. Thorpe displacements; the large instability extending down to 0.31 MPa fills the active mixing layer.

we concentrate on daily cycles of nighttime convective mixing that typically extend to 0.2–0.7 MPa.

In applying the concept of mixed layer to a particular oceanic problem, one must be careful to choose a mixed layer definition that matches the physics of the situation being studied. For instance, models of sea surface temperature (SST) require the diurnal mixing layer, which varies on a daily cycle, because mean SST predicted by assuming the net surface heat flux is evenly distributed throughout the seasonal mixed layer is much lower than SST predicted assuming that during the daytime the added heat is trapped in a shallow surface layer. Further, if for instance one were interested in convection in the atmosphere

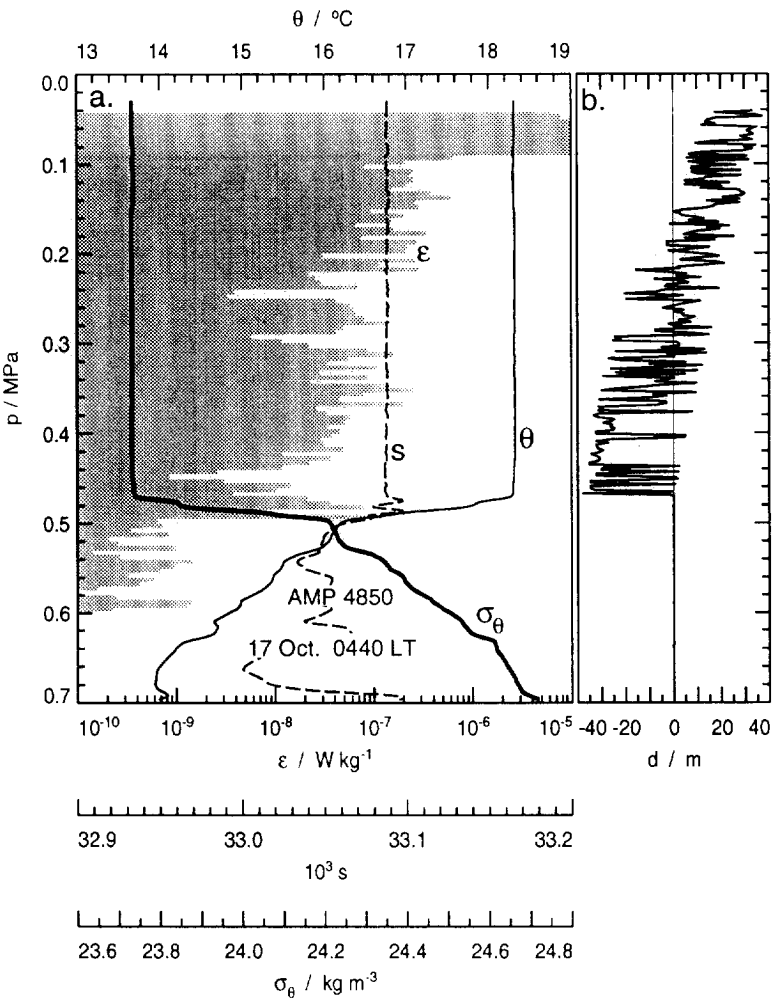

Fig. 2. Profile taken during convective equilibrium on PATCHEX; later in the same night as shown in Fig. 1. Panel a. Profiles of ε, θ, salinity and σ_θ. The shading is ε, estimated in 0.5 m bins: θ and σ_θ have been processed with a 0.8 m triangular filter. Panel b. Thorpe displacements; the instability extending to 0.48 MPa shows active convection reaching the seasonal thermocline.

driven by SST, then the daily cycle in SST would need to be accurately modeled in order to predict the highly nonlinear atmospheric convective response. On the other hand, in the case of momentum fluxes, where there is not a strong direct feedback to the atmosphere, it may be appropriate to use the seasonal mixed layer.

Or consider the case of a phytoplankton bloom: in a rapid bloom with doubling times less than a day (Fuhrman *et al.*, 1985; Prézelin and Ley, 1980), the trapping of a collection of phytoplankton within a shallow surface layer by the diurnal pycnocline could result in a significant increase in production by keeping the newly produced cells within the zone with the most intense light. In a bloom with time scales of several days, this effect would become insignificant as the plankton population would become distributed through the mixed layer

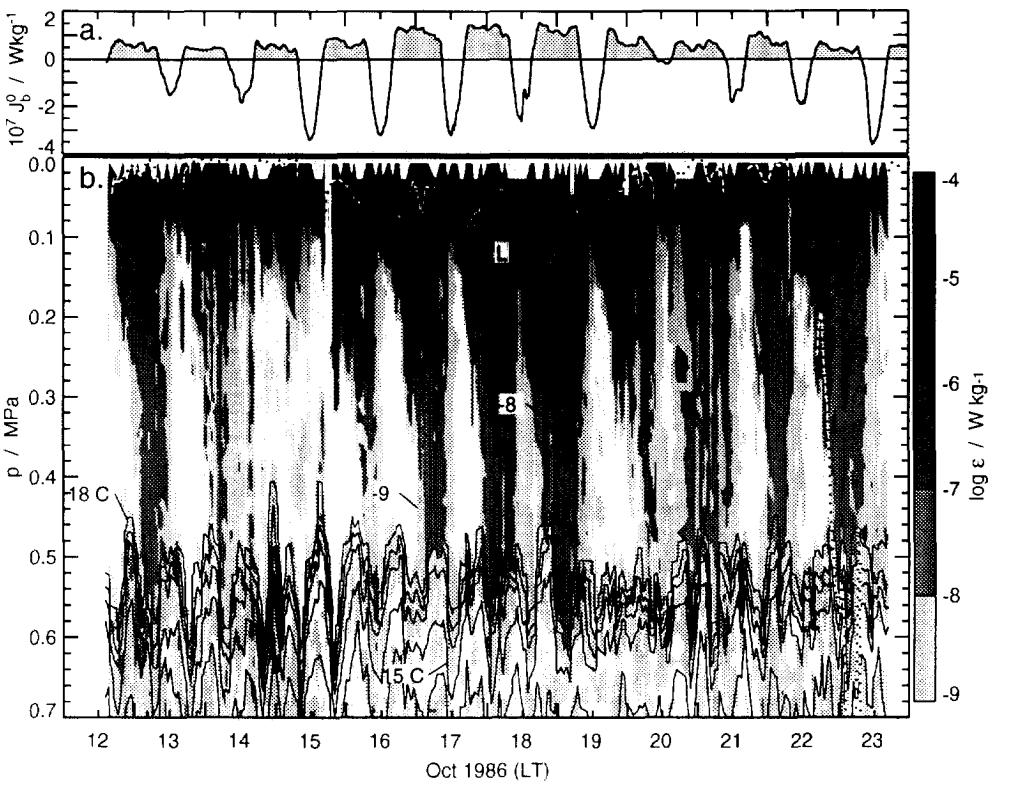

Fig. 3. Summary of turbulent dissipation rates on PATCHEX. Panel a. Surface buoyancy flux J_b^0. Shaded parts mark periods when convection is being forced (cooling). Panel b. Shaded contours are log ε; solid lines are isotherms (1° contour interval), suggesting the depth of the thermocline. Heavy dashed line is Monin-Obukhov length (L), plotted by taking 1 MPa to be equivalent to 100 m.

each night. Thus in studying rapid blooms one would need to consider the diurnal mixed layer cycle, whereas for more slowly growing blooms it would be sufficient to consider only the seasonal mixed layer.

Similarly, gas exchange with the atmosphere and nutrient supply to the surface layer are inhibited during daytime by the suppression of mixing across the diurnal thermocline. Hence consideration of the diurnal mixing cycle may be necessary in quantifying these processes.

When the upper ocean is nearly in thermal equilibrium with the atmosphere on time scales of a few days or more, one can expect a regular daily alternation between convection at night and restratification during the day. The Patches Experiment (PATCHEX), off the coast of California in October 1986, gives a good example (Lombardo and Gregg, 1989; Brainerd and Gregg, 1993a,b). Figure 1 shows a profile taken at 2134 LT (local time), during strong convective forcing (Monin–Obukhov length 5.5 m). The top of the seasonal thermocline is near 0.53 MPa, above which the water column is nearly well-mixed. Between 0.1 MPa and 0.32 MPa ε is generally one or two orders of magnitude greater than

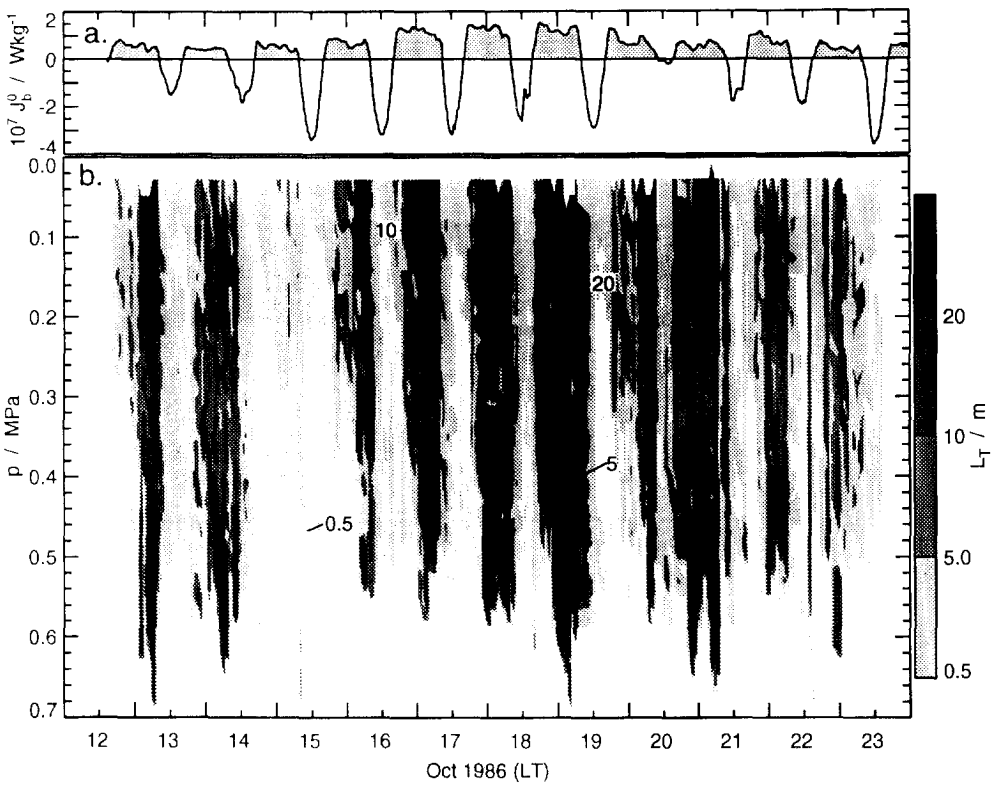

Fig. 4. Summary of turbulent overturning length scales L_T on PATCHEX. Panel a. Surface buoyancy flux J_b^0. Shaded parts mark when convection is being forced (cooling). Panel b. Contours of hour-averages of L_T, in 2 m bins.

the levels observed below 0.32 MPa. At night buoyancy frequency seldom exceeds 0.2 cph, and is often negative. During the day it grows to 1 cph, compared to 12 cph in the seasonal thermocline.

The displacements, d, of water parcels required to re-sort the density profile to achieve static stability (Thorpe, 1977) are shown in panel b; the extent of overturning, matching the region of elevated ε, suggests that there is active overturning extending down to 0.33 MPa. We conclude that convection penetrates to this depth, but not below; note the small density step that corresponds to the bottom of the region of high dissipation. During this period the mixing and mixed layer depths differ. By 0400 LT convection penetrates to the seasonal thermocline, and the diurnal and seasonal thermoclines merge (Fig. 2).

The zone above the seasonal thermocline is not uniformly turbulent through the day, but rather has a strong daily cycle that is evident in the dissipation rate (Fig. 3). Estimating L_T by forming rms averages of the displacements found in the re-sorting process (Panel b of Fig. 1) in 2-m depth bins, we find these values show a pattern very similar to dissipation (Fig. 4). By midnight, convection typically deepens to the seasonal thermocline and has a clear signature in both L_T and dissipation, with ε varying by nearly two orders of magnitude between night and day. Each of these daily deepenings is limited by the

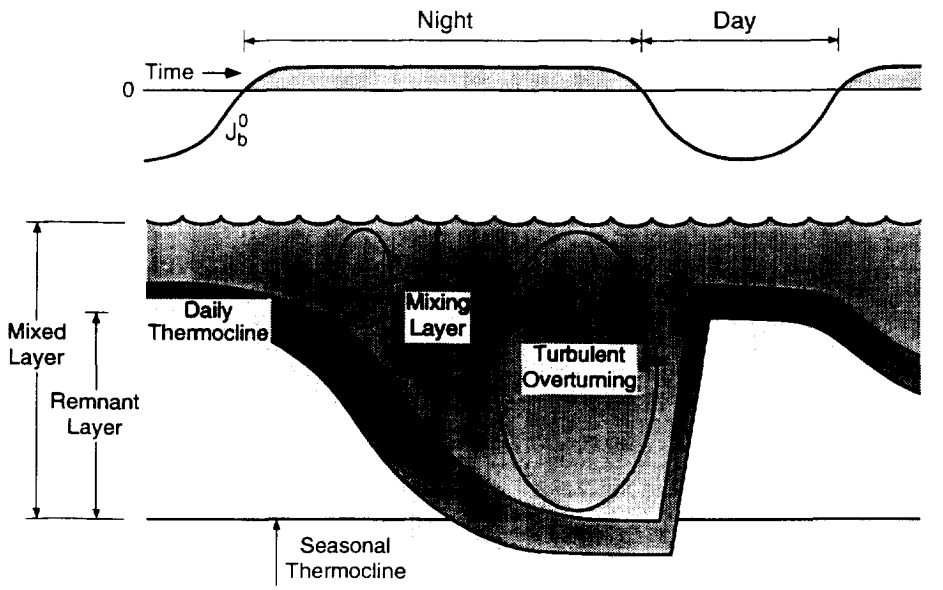

Fig. 5. Diagram showing depth zones in a typical diurnal mixed layer cycle.

seasonal thermocline. In turn, the depth of the seasonal thermocline is the cumulative effect of these convective deepenings.

Thus we distinguish between two concepts of mixed layers, differing in the time scale over which they are mixed (Fig. 5). The *mixing layer* is the depth zone being actively mixed from the surface at a given time and generally corresponds to the depth zone in which there is strong turbulence directly driven by surface forcing. The *mixed layer* is the envelope of maximum depths reached by the mixing layer on time scales of a day or more and is the zone that has been mixed in the recent past. It generally corresponds to the zone above the top of the seasonal pycnocline. The diurnal thermocline corresponds to the entrainment zone, within which the quiescent underlying water is entrained into the actively turbulent region.

During a daily cycle, the mixed layer alternates between well-mixed during nighttime convection and becoming weakly restratified during the day. Figure 6 shows one day's record for θ and ε from the PATCHEX data. At 1600 local time (LT), convective forcing starts, and convection, as seen from the ε record, starts deepening. By 0400 LT convection has reached the top of the seasonal thermocline, and deepening stops. From the θ contours it can be seen that the convective mixing layer generally remains vertically well-mixed throughout. At about 0900 LT the convective forcing ends, and turbulence through most of the depth of the mixed layer starts to decay. Soon thereafter a shallow warm layer begins to form, corresponding to the high turbulence zone near the surface. By 1400 LT the diurnal thermocline is growing in strength, eventually reaching a buoyancy frequency near 4 cph. This growing stratified zone isolates the mixed layer below the mixing layer (the remnant layer) from surface forcing; the remnant layer slowly restratifies during the daytime (Brainerd and Gregg, 1993a).

The weak stratification and absence of overturning within the mixed layer below the diurnal thermocline during daytime suggest that this layer does not remain mixed

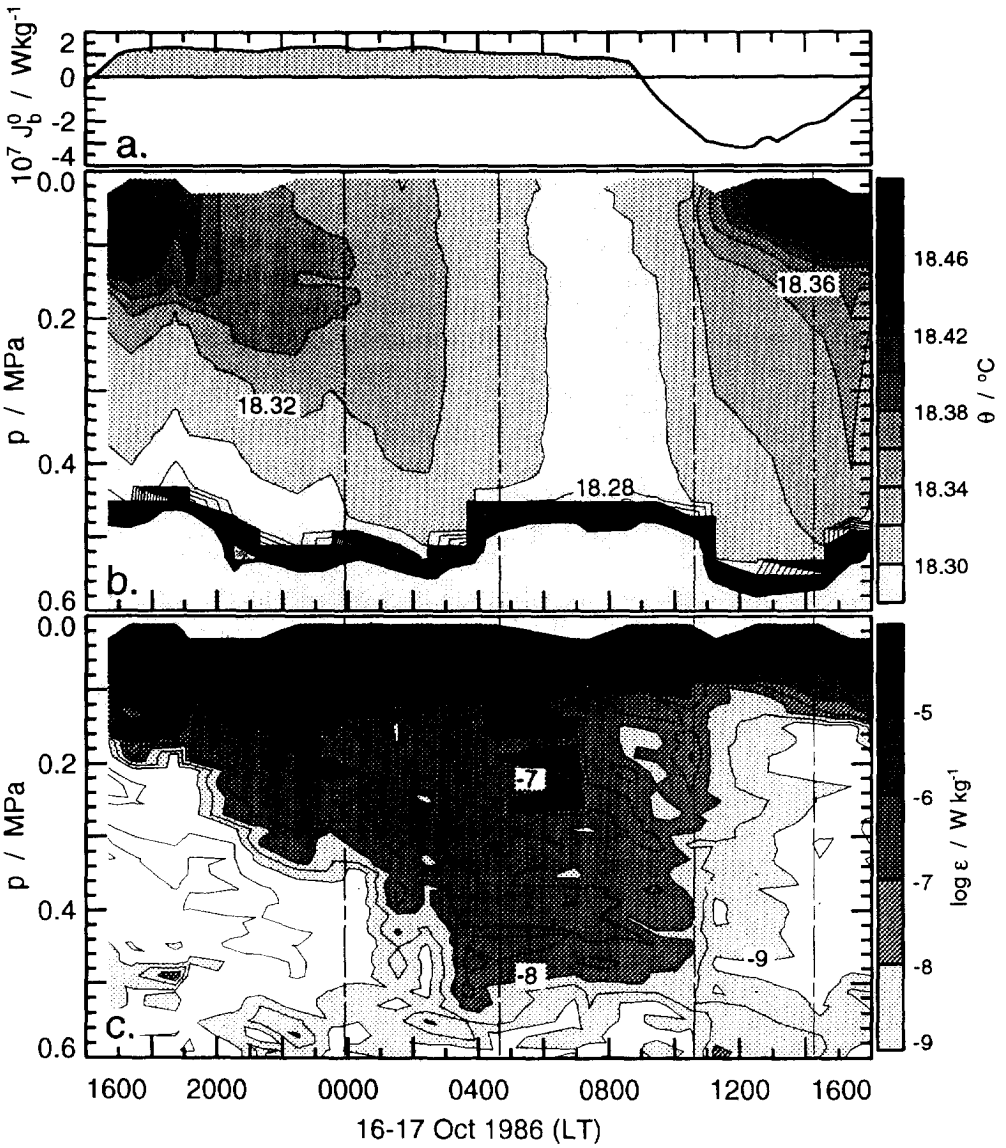

Fig. 6. A one-day cycle from PATCHEX. The vertical dashed lines mark the times of profiles shown in Fig. 7. Panel a. Surface buoyancy flux J_b^0. Panel b. Contours of θ, hour averages in 2 m vertical bins. Contour interval 0.02°C. Heavy black line is the top of the seasonal thermocline. Panel c. Contours of log ε: hour averages in 2 m vertical bins. Contour interval 0.5.

throughout the day. Clearly this is the case for heat added at the surface, and presumably likewise for gasses involved in surface exchanges. Similarly, one would expect plankton to be turbulently mixed within the zone above the diurnal thermocline during daytime, but to become stratified between the diurnal and seasonal thermoclines.

MIXING AND MIXED LAYER DEPTH CRITERIA

In choosing a depth criterion we first must decide which cycle we wish to follow; we particularly need to avoid using a criterion that will sometimes follow one and sometimes another. The depths found by a mixing layer definition should follow the daily cycle in depth to which surface forcings are mixed, while a mixed layer depth definition should follow (on longer time scales) the maximum depths to which mixing recently has penetrated from the surface. Given a time series of dissipation measurements, it is usually quite easy to follow the daily mixing cycle (Fig. 3); in the absence of strong shear, dissipation levels typically decrease by one or two orders of magnitude a few metres below the zone of active convection. Similarly, overturning scales gives a very direct indication of mixing (Fig. 4). However, dissipation rates and overturning scales are difficult to measure; historically mixed and mixing layer depth definitions have of necessity been based on measurements that could be made with a CTD.

Two types of mixed and mixing layer depth definitions have been most commonly used. The first is based on specifying a difference in temperature or density from the surface value; for density

$$\sigma_\theta(D) - \sigma_\theta^0 = (\Delta\sigma_\theta)_C \tag{1}$$

where σ_θ^0 is the value of the surface and $(\Delta\sigma_\theta)_C$ is the specified difference (Wyrtki, 1964; Levitus, 1982; Schneider and Müller, 1990). This type of criterion suffers from difficulties in defining the surface value, particularly during convection, as will be shown below. The second type of criterion is based on specifying a gradient in temperature or density;

$$\frac{\Delta\sigma_\theta}{\Delta z} = \left(\frac{\partial\sigma_\theta}{\partial z}\right)_C \tag{2}$$

where $\Delta\sigma_\theta$ is the difference in σ_θ within a vertical bin of thickness Δz and $(\partial\sigma_\theta/\partial z)_C$ is the specified gradient criterion (Defant, 1936; Bathen, 1972; Lukas and Lindstrom, 1991). This criterion is rather sensitive to the vertical scale over which the (first-differenced) gradients are computed. In this paper, density profiles are vertically averaged in 2 m bins before applying the criteria, approximating the best vertical resolution available from conventional shipborne CTDs, typically limited to salinity spiking and the effects of ship motion (Trump, 1983).

Criteria of both types based on temperature rather than density have been extensively used, as temperature has been easier to measure reliably than density. This works well in many locations, as both the daily and seasonal cycles in surface forcing have large heat fluxes, and weak salt fluxes. However, intense rainfall can produce strongly stratified pools of fresh water that necessitate accounting for salinity in determining both mixed and mixing layer depths (Price, 1979; Lukas and Lindstrom, 1991). In this study, we show illustrations based on density; in the absence of strong salinity gradients, they can be converted easily into equivalent temperature criteria.

Mixing layer depth

While both types of criteria can often correctly find the mixing layer, as identified by dissipation rates, neither type is able to find it completely consistently throughout the daily cycle. We can get an indication of the skill of the different criteria by applying them to a

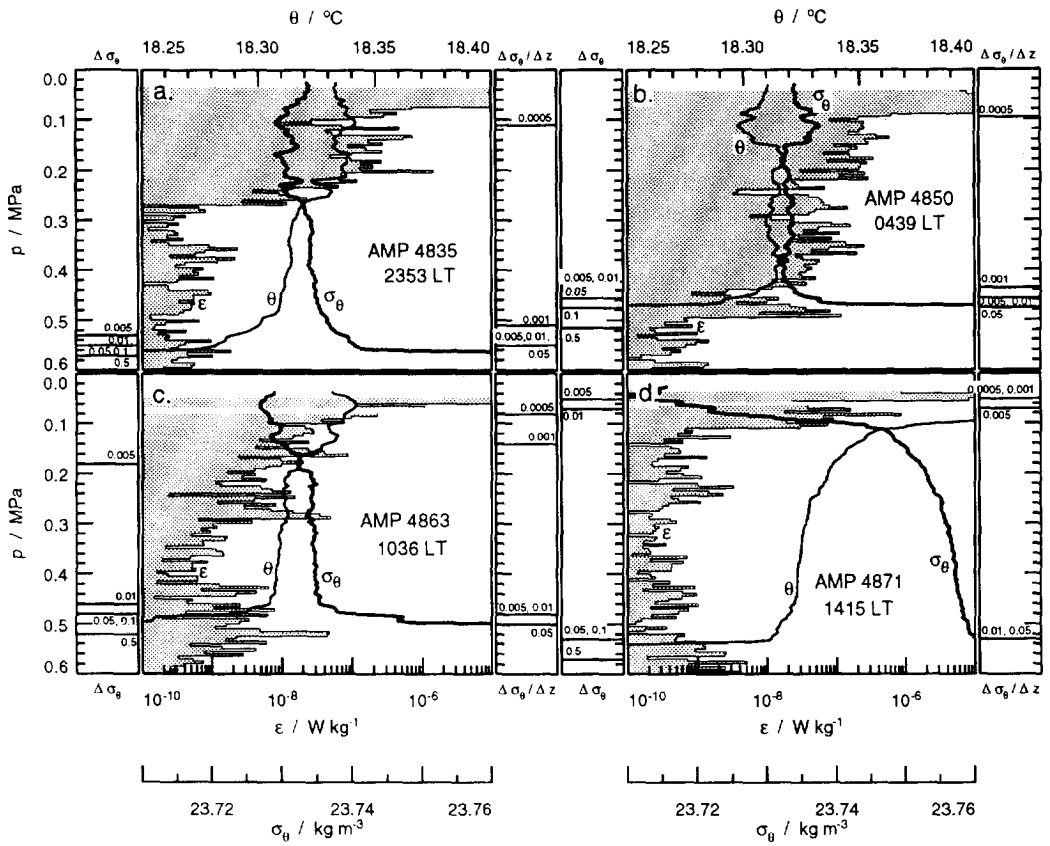

Fig. 7. Profiles of ε, θ and σ_θ taken at four stages of the daily cycle shown in Fig. 6. The shading is ε, estimated in 0.5 m bins; θ and σ_θ have been processed with a 0.8 m triangular filter. Horizontal lines in the side panels mark values returned by the mixed layer depth criteria; density difference criteria on the left hand panels, density gradient criteria on the right. Panel a. Drop 4835; 2353 LT, 16 October 1986, during convective deepening phase. Panel b. Drop 4850; 0439 LT, 17 October 1986, during convective equilibrium phase. Panel c. Drop 4863; 1036 LT, 17 October 1986; start of growth of diurnal thermocline. Panel d. Drop 4871; 1415 LT, 17 October 1986; diurnal thermocline has become quite strong.

series of profiles from PATCHEX. Figure 7 shows profiles taken at four times in the daily cycle shown in Fig. 6. The profile in panel a was taken during convective deepening. From ε, it appears that convection was active down to about 0.26 MPa. The depth range between 0.26 and 0.28 MPa is the entrainment zone, within which ε decreases rapidly, and σ_θ transitions between the nearly unstratified mixing layer above and the stratified remnant layer below. The density and temperature profiles show many overturns within the mixing layer, but the mean has nearly neutral stability; within the entrainment zone σ_θ shows a small increase of about 0.003 kg m^{-3}. This increase is of the same magnitude as the overturns seen above it, and none of the density step depth criteria are able to detect it. A density gradient of $(\Delta\sigma_\theta)_C = 0.005$ kg m^{-4} triggers on an overturn within the mixing layer; larger values of $(\Delta\sigma_\theta)_C$ find the seasonal thermocline. Panel b of Fig. 7 shows a profile taken during the convective equilibrium phase, when convection extends down to the

seasonal thermocline. In this case the mixed and mixing layer depths are the same; all the criteria correctly find the top of the seasonal thermocline, except $(\partial\sigma_\theta/\partial z)_C = 0.0005$. Panel c of Fig. 7 shows a profile taken in the morning, nearly two hours after the end of convective forcing. Below 0.1 MPa the observed dissipation is mostly decaying turbulence from the previous night's convection (Brainerd and Gregg, 1993a). Above 0.1 MPa the diurnal thermocline is starting to form but is still too weak to be detected by many of the proposed criteria. A profile taken a few hours later (Panel d) shows a further decay in the remnant layer turbulence and growth in the strength of the diurnal thermocline. Now more of the proposed criteria are able to identify the depth of the mixing layer. Thus we see that criteria of both types can work in some conditions to find the mixing layer (convective equilibrium phase, or strong daytime diurnal thermocline) but do not work reliably in others (convective deepening phase, or weak daytime diurnal thermocline).

We can see the results of the problems described above by comparing overturning length scales with the depths picked out by the proposed mixed layer definitions (Fig. 8). Panel a includes the criteria based on a density difference from the surface value, using density profiles that have been averaged into 2 m bins. Criteria using $(\Delta\sigma_\theta)_C = 0.005$ and 0.01 follow the daily cycle of turbulence rather well. Panel b shows the criteria based on density gradients. None of the gradient criteria follow the daily cycle; $(\partial\sigma_\theta/\partial z)_C = 0.01$ and 0.05 follow the seasonal thermocline, while the smaller gradients sometimes find the base of the mixing layer, but just as often are triggered by overturns within the layer.

Finding mixing layer depths during the convective deepening phase is particularly problematic. Figure 9 shows profiles taken on four consecutive drops about 15 minutes apart, during the convective deepening phase of the night shown in Fig. 8. In each case the depth to which convection is active is unambiguously indicated by the sharp cutoff in dissipation rate at around 0.3 MPa, but the different depth criteria give widely varying results, with large variability between density difference and gradient criteria on a given drop, and great variability from drop to drop using a single criterion.

Each of these drops shows to some degree a condition often seen during convection: cold water formed at the surface forms a shallow pool of dense water, typically much denser than any other water within the mixing layer (Gregg, 1987; Anis and Moum, 1992). This presents a problem for a density (or temperature) difference criterion, which in such cases will clearly be unable to pick out the mixing layer depth if they are looking for a specified density increase with respect to the surface value. A density difference of $(\Delta\sigma_\theta)_C = 0.005$ works quite well on the first drop of Fig. 9, but not on any of the other drops. It would have worked reasonably well on the three other drops if the dense surface water were removed from the profiles. Gradient criteria $(\partial\sigma_\theta/\partial z)_C = 0.0005$ and 0.001 triggered on a shallow overturn in the first profile, and did rather well in the second. In the third drop, $(\partial\sigma_\theta/\partial z)_C = 0.0005$ triggered on a small overturn within the mixing layer; the density gradient picked out by $(\partial\sigma_\theta/\partial z)_C = 0.001$ may mark the top of the entrainment zone, but convection is clearly active nearly 10 m deeper, as seen in the dissipation profile. In the fourth profile, it is $(\partial\sigma_\theta/\partial z)_C = 0.0005$ that picks out the top of the entrainment zone, while $(\partial\sigma_\theta/\partial z)_C = 0.001$ finds the bottom of active convection.

Thus we see there is no criterion that works consistently with these drops; there is typically a density step of 0.0025–0.005 kg m^{-3} corresponding to the depth at which ε strongly decreases, but without the ε data it would often be difficult to pick out which density step is the right one. There is also typically a distinct change in the character of the density profile at this point, with numerous overturns with length scales between a meter

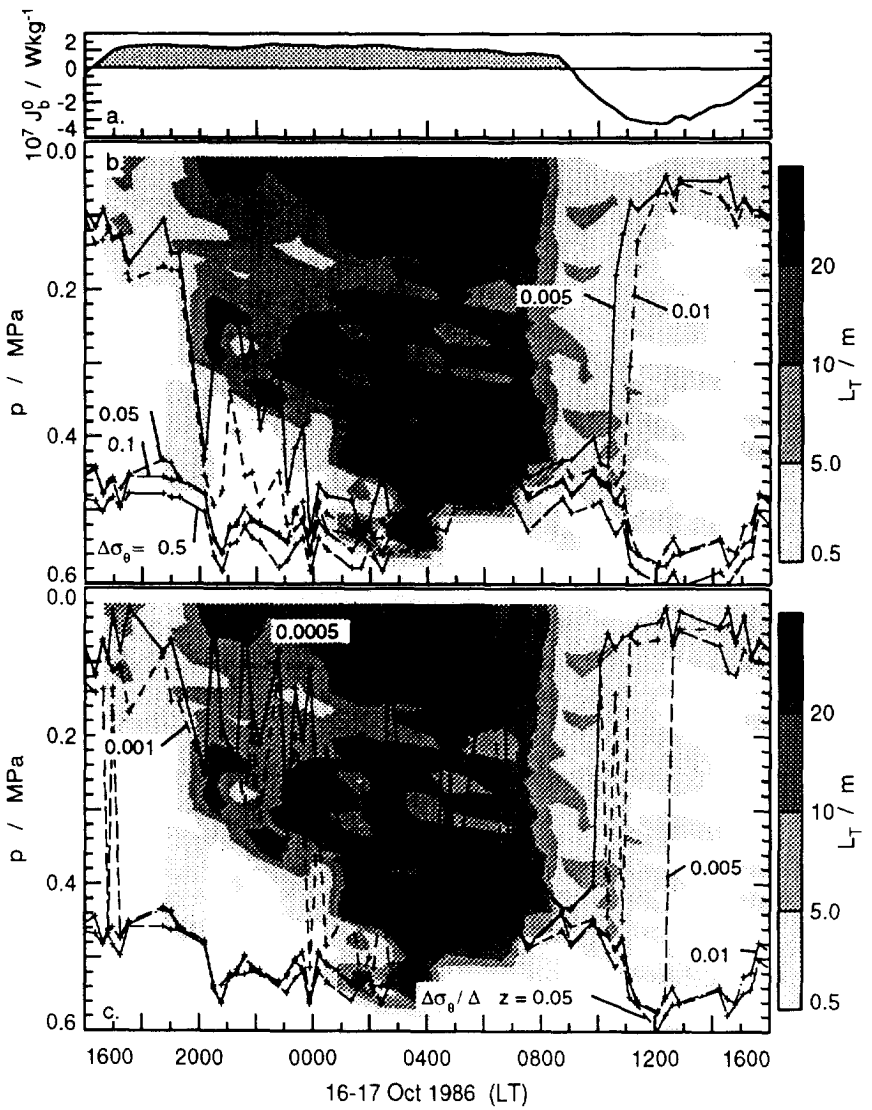

Fig. 8. Comparison of contours of L_T with mixed layer depths by various definitions, for a daily cycle (16–17 October 1986) during PATCHEX. Panel a. Surface buoyancy flux J_b^0. Panel b. Shaded contours are L_T; lines are the density difference criteria. Panel c. Shaded contours are L_T; lines are the density gradient criteria.

and the depth of the mixing layer. However, most of these overturns would not be visible in data with resolution coarser than 1 m, and hence are not a useful indicator for use with normal CTD data.

We observed rather different conditions on the pilot cruise of the Coupled Ocean Atmosphere Response Experiment (COARE), which included 17 days of microstructure measurements at 147°E, 0°N and 5 days at 147°E, 2°N (Brainerd and Gregg, 1991). An overview of the equatorial time series (Fig. 10) emphasizes the importance of the

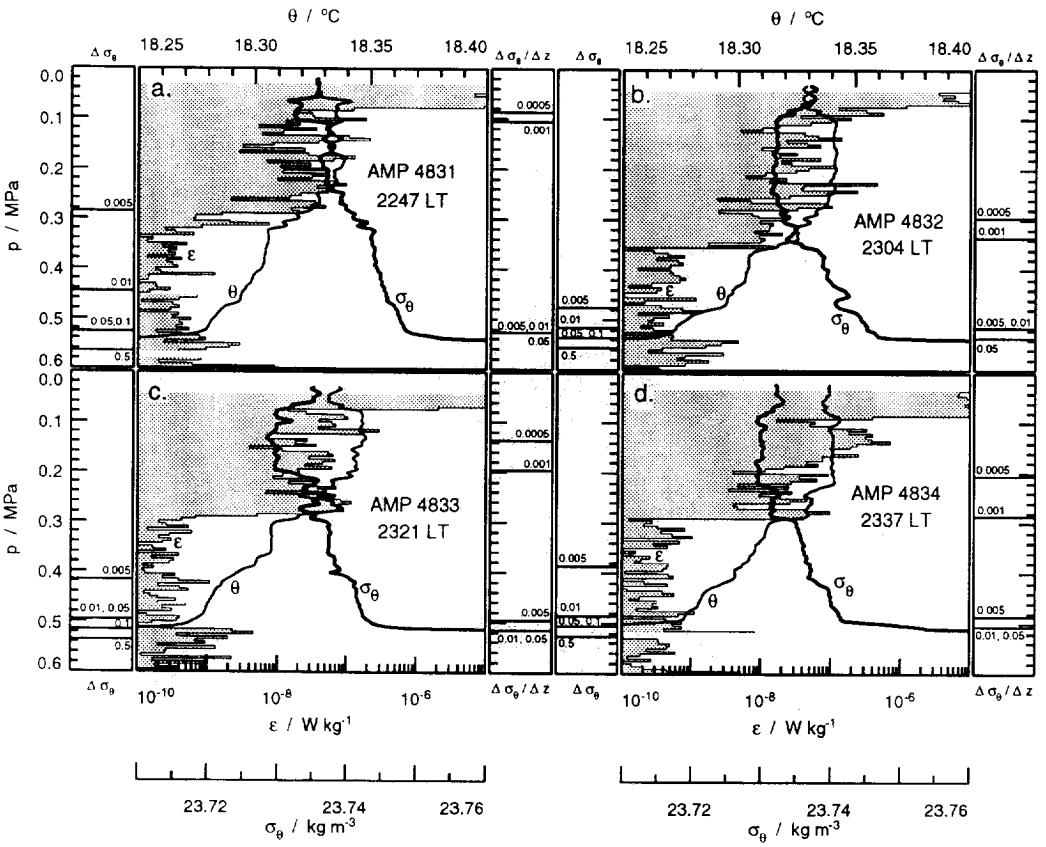

Fig. 9. Profiles of ε, θ and σ_θ from four consecutive drops during convective deepening on 16 October, from PATCHEX. The shaded line is ε, estimated in 0.5 m bins; θ and σ_θ have been processed with a 0.8 m triangular filter. Horizontal lines in the side panels mark values returned by the mixed layer depth criteria; density difference criteria on the left hand panels, density gradient criteria on the right. Panel a. Drop 4831; 2247 LT. Panel b. Drop 4832; 2304 LT. Panel c. Drop 4833; 2321 LT. Panel d. Drop 4834; 2337 LT.

distinction between the mixing and mixed layers. Judging the mixing layer depth from ε, it can be seen that the mixing depth is highly variable from one night to the next, reaching maximum depths between 0.2 and 0.7 MPa, and only occasionally extends down to the seasonal thermocline, the top of which is near 0.7 MPa; the depth of the top of the seasonal thermocline is set only by occasional deep mixed layer events. The strong day to day variability in mixing layer depth appears to be related to the strong remnant layer stratification (Fig. 11) that usually prevents convection from penetrating to the seasonal thermocline at night.

In order to show the overall performance of the two types of criteria, Fig. 12 compares the range of mixed layer depth definitions with the observed overturning for one typical day. As in the PATCHEX case (Fig. 8), the density difference criteria $(\Delta\sigma_\theta)_C = 0.005$ and 0.01 follow the daily mixing cycle reasonably well, while none of the other criteria do.

In this cruise the surface forcing was dominated by squalls, which frequently included very heavy rainfall. This emphasizes the possible importance of salinity to mixed layers;

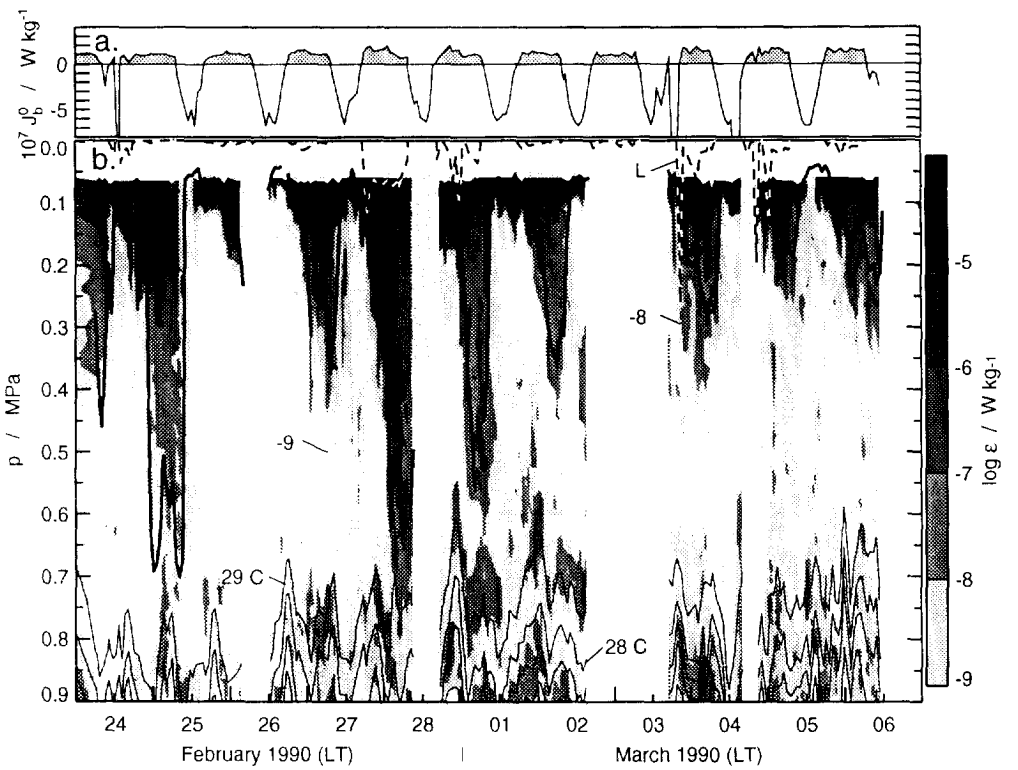

Fig. 10. Overview of 11 days of the COARE pilot cruise data. LT is local time (UTC + 10 h). Panel a. Surface buoyancy flux J_b^0. The large negative extrema are due to episodes of rainfall. Panel b. Contours of hour-averages of ε, in 2 m vertical bins. The heavy line is the hour-averaged depth at which σ_θ exceeds the surface value by 0.01 kg m^{-3}. The thin solid lines are contours of hour-averaged θ (contour interval is 1.0°C), suggesting the depth of the seasonal thermocline. Dashed line is Monin-Obukhov length (L), plotted by taking 1 MPa to be equivalent to 100 m.

pools of fresh water left at the surface by rain often have strong haloclines at their base; the resulting pycnocline strongly suppresses mixing. The profile shown in Fig. 13 was taken a few hours after heavy rain; from ε and σ_θ it can be seen that the depth of the mixing layer is 0.29 MPa; the only indication of this depth from the θ profile is that there are overturns visible with length scales of a few meters above that, and no overturns below. These overturns are too small to be seen in data taken with a conventional CTD. Thus the mixing layer depth could not be identified by temperature measurements alone (Lukas and Lindstrom, 1991).

By comparing the depths returned by each of the criteria to mixing layer depths determined subjectively from density, dissipation rate, and Thorpe displacement profiles, we can get some idea of how well the criteria work with the PATCHEX and COARE data (Table 1). The PATCHEX data require smaller values than the COARE data for both $(\Delta\sigma_\theta)_c$ and $(\partial\sigma_\theta/\partial z)_c$ in order to match the subjectively determined depths, apparently because of the weaker stratification within the remnant layer in the PATCHEX data. The rms differences between the depths found subjectively and those returned by the criteria

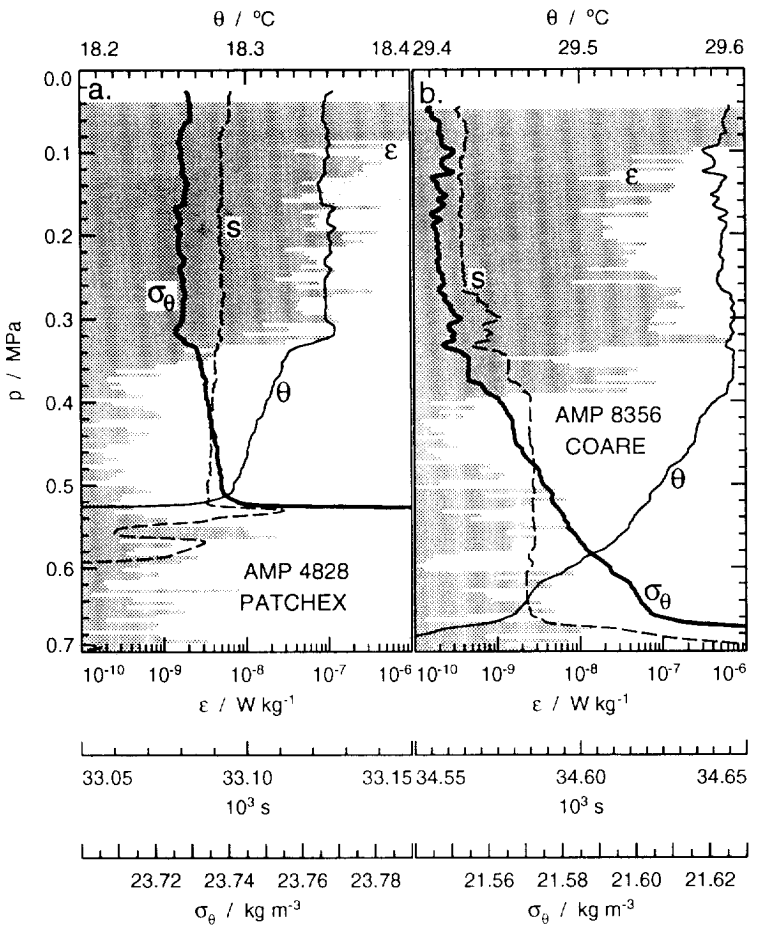

Fig. 11. Comparison of profiles taken during convective deepening on PATCHEX (Panel a) and COARE (Panel b). Remnant layer stratification is much longer in the COARE data.

are smaller for the optimal $(\Delta\sigma_\theta)_C$ values than those for the optimal $(\partial\sigma_\theta/\partial z)_C$ values (0.056 MPa vs 0.076 MPa for COARE).

Turbulence is not always a good indicator of mixing layer depth. The *Tropic Heat I* cruise, in November and December 1984 at 140°W in the equatorial Pacific, shows a strong contrast with the preceding data sets. Here on most nights there is convective forcing at the surface; the mixing layer (as defined by $(\Delta\sigma_\theta)_C = 0.01$) deepens from about 0.1 MPa to about 0.3 MPa. Below that, extending down to 2 or 3 times the mixing layer depth, the observations show strong turbulent episodes, often with ε higher than in the mixing layer (Fig. 14). These deep events typically start when convection has become well-established, and continue through the rest of the night and into the following morning. Gregg *et al.* (1985) and Moum *et al.* (1989) have suggested that convective plumes impinging on the bottom of the mixing layer generate internal waves that propagate downwards into a region of low Richardson number; the resulting increased shear may be enough to give sub-critical Richardson numbers, leading to shear instabilities and turbulence.

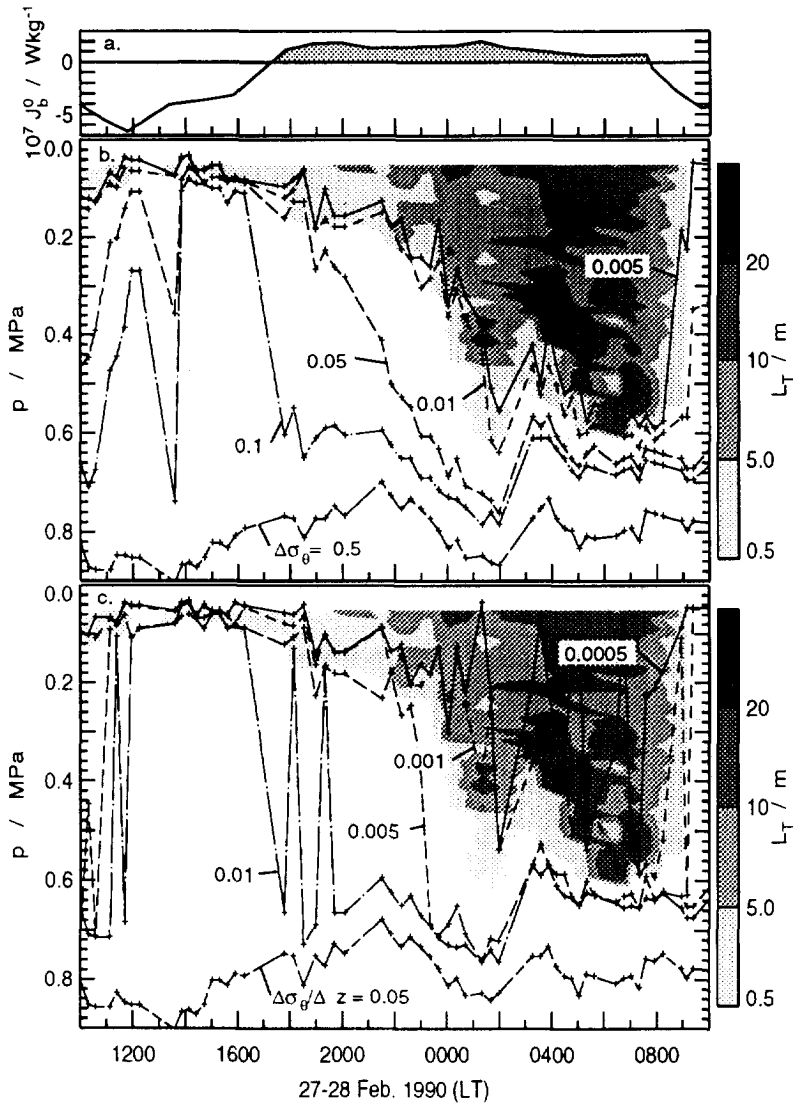

Fig. 12. Comparison of contours of L_1 with mixed layer depths by various definitions, for a daily cycle (27–28 Feb. 1990) during the COARE pilot cruise. Panel a. Surface buoyancy flux J_b^0. Panel b. Shaded contours are L_1; lines are the density difference criteria. Panel c. Shaded contours are L_1; lines are the density gradient criteria.

Figure 15 shows a profile taken during strong deep turbulence. From θ and σ_θ it is clear that the mixed layer depth is no greater than 0.25 MPa; strong turbulence extends down to 0.7 MPa, where it drops by an order of magnitude in a 3 m depth bin. In this case there is a continuous zone of turbulence with a magnitude similar to the surface buoyancy flux extending far below a well-defined mixed layer. This example points out the hazard in identifying the mixing layer depth as the depth to which strong turbulence extends from the surface. The difference between the mixing layer and the turbulent layer below can be

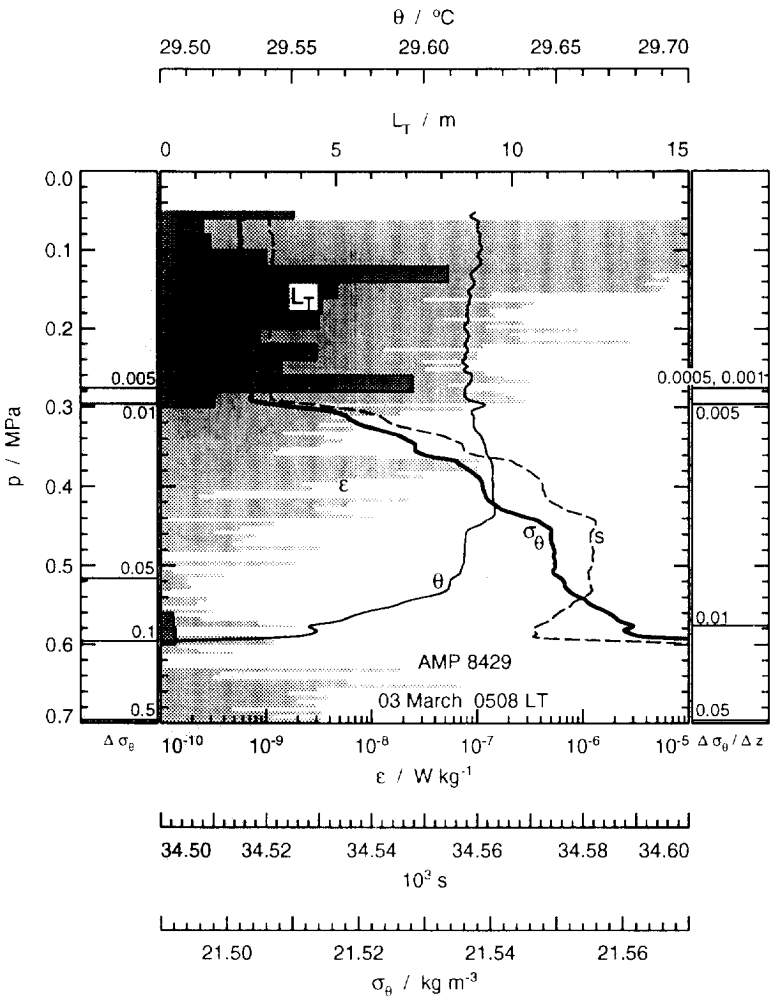

Fig. 13. Profiles from the COARE pilot cruise: θ, σ_θ, salinity and ε. At 0.29 MPa the strong halocline gives a strong pycnocline; ε drops an order of magnitude at the same depth. Thus this appears to mark the bottom of the mixing layer, although there is very little indication of that in θ.

seen in L_T, which shows overturns spanning the mixing layer, while below that the overturns are smaller than 2 m. Within the mixing layer the overturning length scale is set by static instabilities due to convection. From the density profile it is clear that convection does not extend below 0.25 MPa; overturning below that must be the result of different processes.

We generally identify the mixing layer with high turbulence not so much because the turbulence is controlling the mixing layer dynamics, but rather because the processes that do control mixing layer deepening, such as penetrative convection, have a strong signature in turbulence. The Tropic Heat data provide an example suggesting that there are other processes that also generate turbulence, but which do not form a mixed layer.

Table 1. Summary of differences between depths found by mixing layer depth definitions (D_{obj}) and mixing layer depths determined subjectively (D_{subj}), for PATCHEX and COARE data. ΔD is $\langle D_{subj} - D_{obj} \rangle$, averaged over all drops in which both D_{subj} and D_{obj} exceed 0.1 MPa; ΔD_{RMS} is rms difference; n is the number of good samples

Criterion	ΔD MPa	ΔD_{RMS} MPa	n
PATCHEX			
$(\Delta\sigma_\theta)_C = 0.005$	−0.023	0.075	378
0.010	−0.072	0.113	386
0.050	−0.159	0.212	387
0.100	−0.167	0.219	387
0.500	−0.198	0.244	387
$(\partial\sigma_\theta/\partial z)_C = 0.0005$	0.033	0.095	224
0.0010	−0.015	0.096	331
0.0050	−0.144	0.200	387
0.0100	−0.159	0.214	387
0.0500	−0.171	0.223	387
COARE			
$(\Delta\sigma_\theta)_C = 0.005$	0.003	0.056	618
0.010	−0.024	0.058	671
0.050	−0.144	0.189	738
0.100	−0.260	0.298	740
0.500	−0.582	0.597	740
$(\partial\sigma_\theta/\partial z)_C = 0.0005$	0.053	0.093	383
0.0010	0.013	0.063	532
0.0050	−0.110	0.184	697
0.0100	−0.209	0.279	733
0.0500	−0.636	0.663	740

Mixed layer depth

Mixed layer depths are often much more easily determined than mixing layer depths, as the signal is much stronger. For example, in the PATCHEX data, criteria based upon $(\Delta\sigma_\theta)_C = 0.05$, 0.1 and 0.5 and upon $(\partial\sigma_\theta/\partial z)_C = 0.01$ and 0.05 all find the top of the seasonal thermocline rather consistently (Fig. 8); in this case, where nighttime convection regularly penetrates to the seasonal thermocline, this depth corresponds to the mixed layer depth. Note that the top of the seasonal thermocline is heaving through a depth range of 10–20 m with a semidiurnal frequency (Fig. 3; also Fig. 10 for the COARE data). Thus to get an unbiased estimate of mixed layer depth, the observations must extend over a tidal cycle.

The COARE data is considerably more ambiguous, particularly in periods such as days 62–65 (Fig. 10) during which the mixing layer does not regularly penetrate down to the seasonal thermocline. During such times the region between the deepest convective penetration and the top of the seasonal thermocline appears to go for several days without being mixed. A typical profile from this period (Fig. 16) shows the top of the seasonal thermocline near 0.75 MPa, although the previous night's convection reached no deeper than 0.3 MPa. There is considerable stratification in the region between 0.3 and 0.75 MPa,

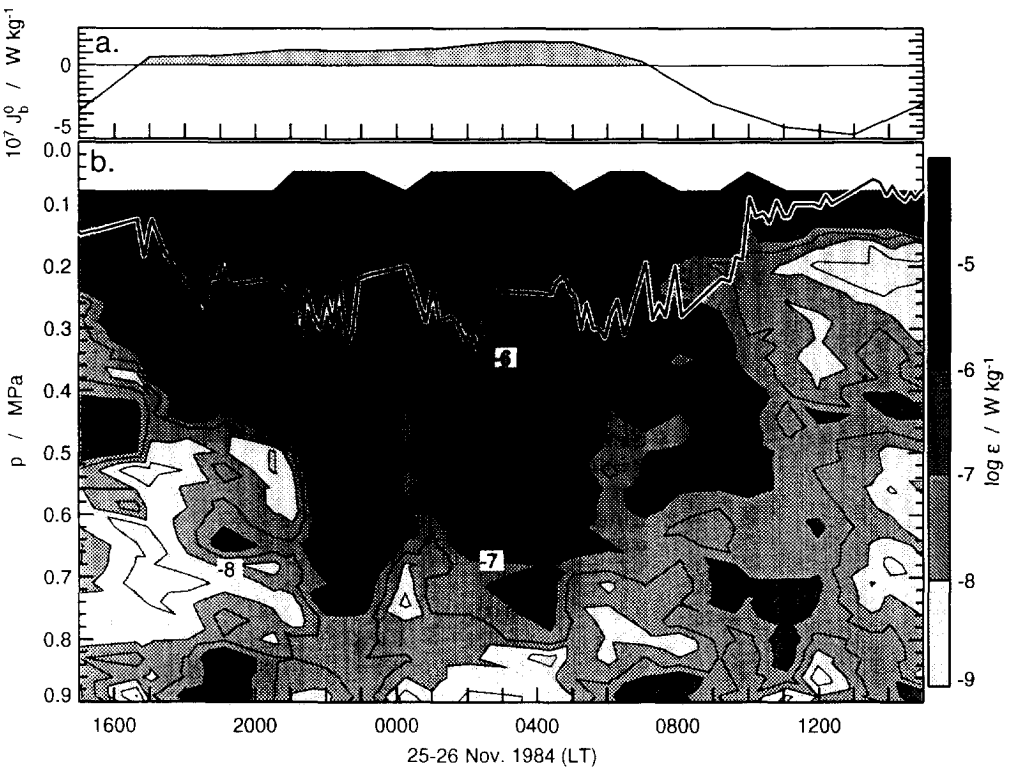

Fig. 14. A one-day cycle from the Tropic Heat Cruise. LT is local time (UTC—9 h). Panel a. Surface buoyancy flux J_b^0. Panel b. Contours of log ε, and mixing layer depth found using ($\Delta\sigma_{\theta y c}$ = 0.01 (white line), for a one-day cycle from the Tropic Heat Cruise. LT is local time (UTC—9 h). During convection, elevated dissipation rates extend from the surface down to depths exceeding three times the mixing layer depth.

with buoyancy frequencies around 4 cph from 0.3 to 0.5 MPa, increasing to a maximum of near 20 cph at the top of the seasonal thermocline. It is not clear *a priori* whether or not one should call this region a mixed layer. Presumably the observed depth of the seasonal thermocline was set by previous mixed layer events, but one working in a context of processes with time scales less than a few days would perhaps want to use the depth of the remnant layer from the previous night's convection as the mixed layer.

DISCUSSION

In many conditions our observations show a strong daily cycle in surface layer mixing, with nighttime convection driving active mixing from the surface to the seasonal thermocline, and daytime restratification within the remnant layer. Thus we are led to define both a mixing layer, which is actively being mixed, and a mixed layer, which is the result of the recent history of mixing layers. The distinction is significant, because it is often important to match the mixed layer time scale to that of the process being studied. While the mixed layer depth is often unmistakably marked by the top of the seasonal thermocline, the

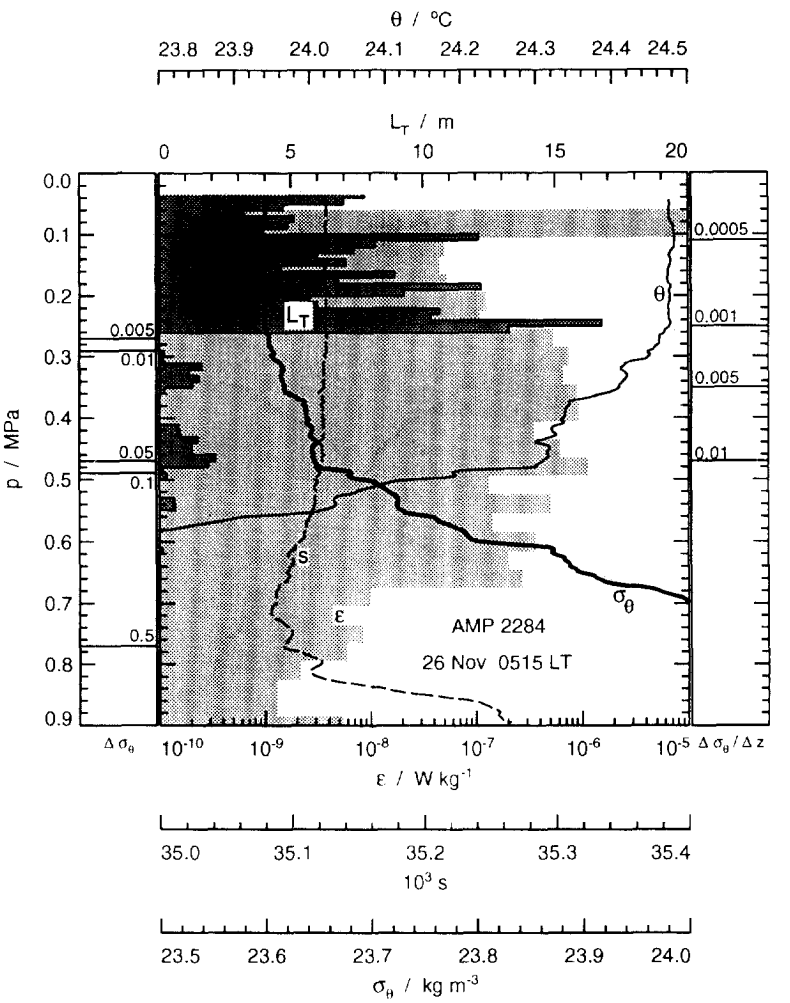

Fig. 15. Profile from the Tropic Heat Cruise; θ (thin solid line), σ_θ (heavy solid line), salinity (dashed line), and ε (shaded). θ and σ_θ are well-mixed down to 0.2 MPa, although strong turbulence extends past 0.8 MPa.

mixing layer depth is typically marked only by a small step in temperature or density, often of magnitude similar to that of overturns within the mixing layer.

The mixing layer depth can best be determined from measurements of overturning length scales, which are perhaps the most direct measure of active mixing processes. Overturning length scales within a convecting layer are dominated by static instabilities resulting from cold water in the surface layer and give a good indication of the maximum depth to which the convection can penetrate. However, there are some problems with determining mixing layer depths from L_T. Due to the intermittence of turbulence, a single profile can give quite misleading results. Also, conventional shipborne CTDs are typically not capable of resolving these overturns, largely due to the effects of ship motions (Fig. 17). De-coupling the CTD from ship motions, either by lowering from a fixed platform

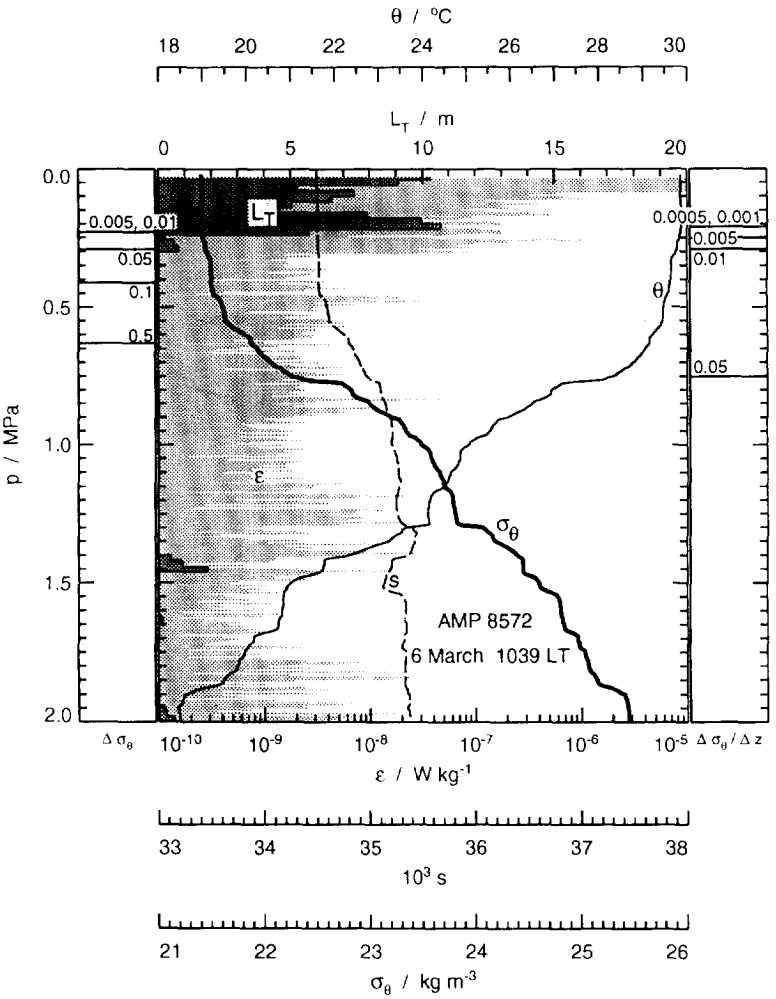

Fig. 16. Profile from the COARE pilot cruise; θ (thin solid line), σ_θ (heavy solid line), salinity (dashed line), and ε (shaded). The top of the seasonal thermocline is near 0.75 MPa, but maximum nighttime convective penetration is to less than 0.3 MPa.

(e.g. FLIP, or ice floes) or by using a free-falling instrument (Fig. 18), may improve resolution sufficiently to allow identification of the mixing layer.

The processes driving mixing also have a clear signal in dissipation. Where convection is active, dissipation rates are high, often decreasing by an order of magnitude per metre at the base of the mixing layer. However, there are also other processes with high dissipation rates that do not form mixed layers (e.g. in the central equatorial Pacific), so at times dissipation measurements alone are insufficient.

We applied the standard types of mixed layer definitions to our data, i.e. density difference from the surface value, and density gradient, using a range of values for each. The density difference criteria proved more stable than the gradient criteria; we find values of $(\Delta\sigma_\theta)_C = 0.005$ and 0.01 kg m^{-3} give the best results for determining mixing layer

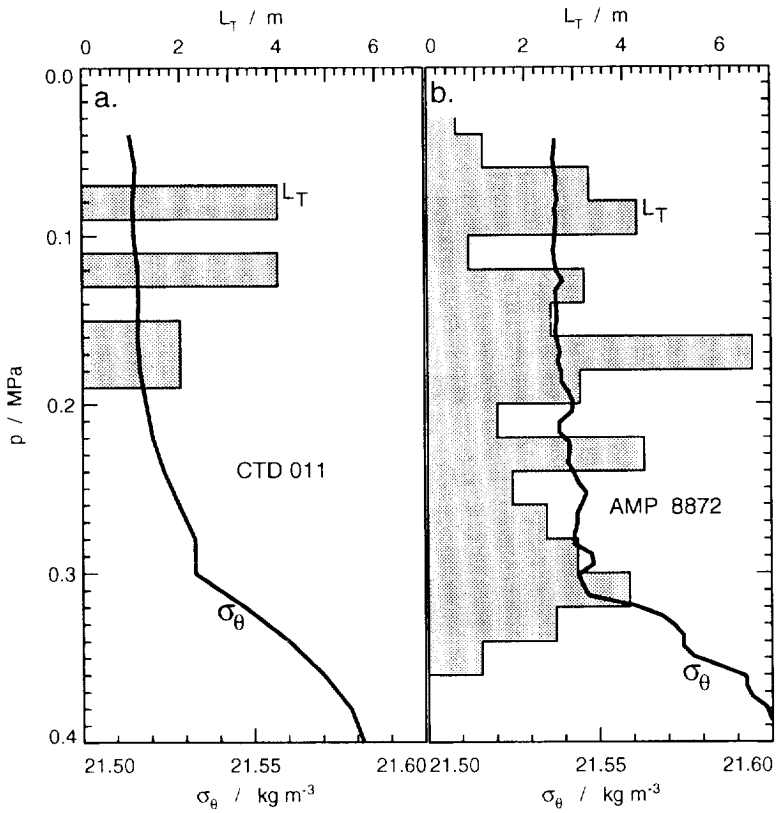

Fig. 17. Comparison of profiles taken within an hour period on the COARE pilot cruise, with a conventional CTD (panel a.) and AMP (panel b.). CTD profile includes only data taken during increasing pressure. The AMP σ_θ profile shows continuous overturning down to about 0.35 MPa, with L_T of 3–4 m; the CTD profile shows almost no overturns.

depths. For the PATCHEX data, values of $(\Delta\sigma_\theta)_C = 0.05$ to 0.5 kg m^{-3} return the mixed layer depth. For the COARE data, with stronger restratification in the remnant layer, $(\Delta\sigma_\theta)_C$ needed to be at least 0.5 kg m^{-3} in order to find the mixed layer. For the gradient criteria, values of $(\partial\sigma_\theta/\partial z)_C$ of 0.0005 and 0.001 kg m^{-4} worked best for finding the mixing layer, although the former sometimes triggered on overturns within the mixing layer, and the latter sometimes found the mixed layer depth instead. Values of $(\partial\sigma_\theta/\partial z)_C$ of 0.01 and 0.05 kg m^{-4} consistently found the PATCHEX mixed layer depth, while only 0.05 kg m^{-4} worked for the COARE data.

Finally we conclude that although both the density difference and density gradient criteria are able to find the mixed layer depth rather well, neither type consistently returns the mixing layer depth. It appears the best way to find mixing layers is from measurements that resolve the turbulent overturns within the mixing layer.

Acknowledgements—The National Science Foundation and the Office of Naval Research funded collection of these data. The analysis was supported by the "Mixing to Mesoscale" University Research Initiative. We thank Ren-Chieh Lien, Hemantha Wijesekera, and Paulette Struckman for many stimulating discussions, and two

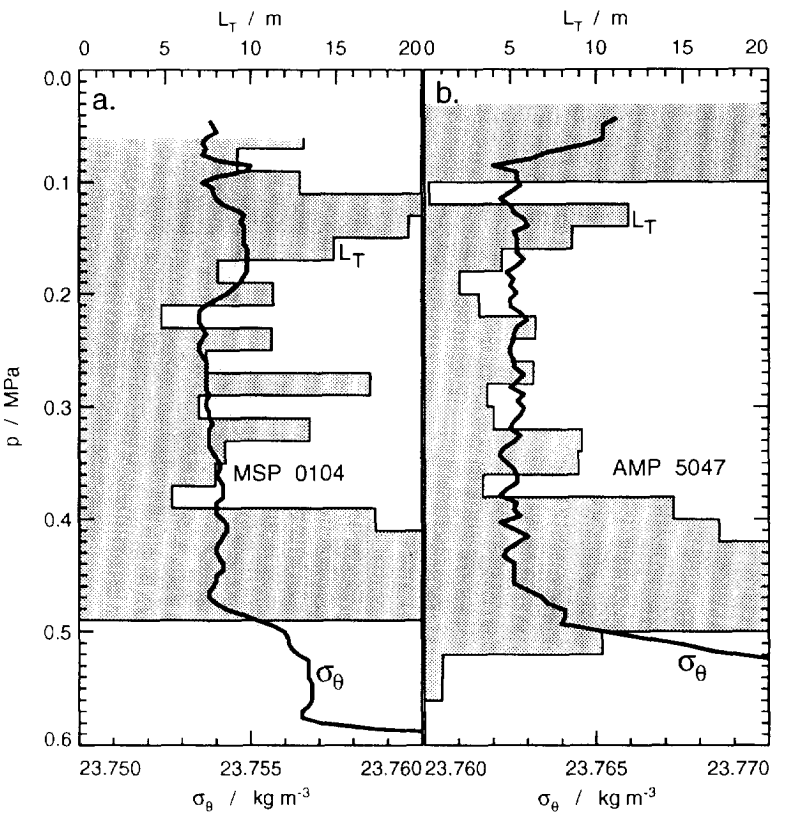

Fig. 18. Comparison of profiles taken within an hour period on PATCHEX, with MSP, (panel a) a free-falling instrument with Sea-Bird sensors, similar to those on a conventional CTD, and with AMP (panel b). Both profiles show continuous overturning from the surface down to about 0.5 MPa.

anonymous reviewers for helpful comments. Contribution 2145 of the School of Oceanography, University of Washington.

REFERENCES

Anis A. and J. N. Moum (1992) The superadiabatic surface layer of the ocean during convection. *Journal of Physical Oceanography*, **22**, 1221–1227.

Bathen K. H. (1972) On the seasonal changes in the depth of the mixed layer in the North Pacific Ocean. *Journal of Geophysical Research*, **77**, 7138–7150.

Brainerd K. E. and M. C. Gregg (1991) Preliminary results of the COARE microstructure pilot. *TOGA Notes*, **4**, 1–4.

Brainerd K. E. and M. C. Gregg (1993a) Diurnal restratification and turbulence in the oceanic surface mixed layer—Part 1: Observations. *Journal of Geophysical Research*, **98**, 22,645–22,656.

Brainerd K. E. and M. C. Gregg (1993b) Diurnal restratification and turbulence in the oceanic surface mixed layer—Part 2: Modeling. *Journal of Geophysical Research*, **98**, 22,657–22,664.

Defant A. (1936) Die Troposphäre des Atlantischen Ozeans. In: *Schichtung und zierkulation des Atlantischen Ozeans*, Wissenschaftliche Ergebnisse der Deutschen Atlantischen Expedition auf dem Forschungs- und Vermessungsschiff "*Meteor*" 1925–1927, **6**, 1. Teil.

Fuhrman J. A., R. W. Eppley, A. Hagström and F. Azam (1985) Diel variations in bacterioplankton,

phytoplankton, and related parameters in the Southern California Bight. *Marine Ecology Progress Series*, **27**, 9–20.

Gregg M. C. (1987) Structures and fluxes in a deep convecting mixed layer. In: *Dynamics of the Oceanic Surface Mixed Layer, Proceedings, Hawaiian Winter Workshop*. P. Müller and D. Henderson, editors, Hawaii Institute of Geophysics, Honolulu, pp. 1–24.

Gregg M. C., H. Peters, J. C. Wesson, N. S. Oakey and T. J. Shay (1985) Intensive measurements of turbulence and shear in the equatorial undercurrent. *Nature*, **318**, 140–144.

Levitus S. (1982) Climatological Atlas of the World Ocean, *NOAA Prof. Pap.*, **13**, National Oceanic and Atmospheric Administration, Rockville Md, 173 pp.

Lombardo C. P. and M. C. Gregg (1989) Similarity scaling during nighttime convection, *Journal of Geophysical Research*, **94**, 6273–6284.

Lukas R. and E. Lindstrom (1991) The mixed layer of the western equatorial Pacific Ocean. *Journal of Geophysical Research*, **96**, 3343–3357.

Moum J. N., D. R. Caldwell and C. A. Paulson (1989) Mixing in the equatorial surface layer and thermocline, *Journal of Geophysical Research*, **94**, 2005–2021.

Osborn T. R. (1980) Estimate of the local rate of vertical diffusion from dissipation measurements, *Journal of Physical Oceanography*, **10**, 83–89.

Prézelin B. B. and A. C. Ley (1980) Photosynthesis and chlorophyll *a* fluoresence rhythms of marine phytoplankton. *Marine Biology*, **55**, 295–307.

Shay T. J. and M. C. Gregg (1986) Convectively driven turbulent mixing in the upper ocean. *Journal of Physical Oceanography*, **16**, 1777–1798.

Schneider N. and P. Müller (1990) The meridional and seasonal structures of the mixed-layer depth and its diurnal amplitude observed during the Hawaii-to-Tahiti Shuttle Experiment. *Journal of Physical Oceanography*, **20**, 1395–1404.

Thorpe S. A. (1977) Turbulence and mixing in a Scottish loch. *Philosophical Transactions of the Royal Society of London, Series A*, **286**, 125–181.

Trump C. L. (1983) Effect of ship's roll on the quality of precision CTD data, *Deep-Sea Research*, **30**, 1173–1183.

Woods J. D. and W. Barkmann (1986) The response to the upper ocean to solar heating. I: The mixed layer. *Quarterly Journal of the Royal Meteorological Society*, **112**, 1–27.